

# Visualizing PI3 Kinase-Mediated Cell-Cell Signaling during *Dictyostelium* Development

Dirk Dormann,<sup>1</sup> Gerti Weijer,<sup>1</sup> Carole A. Parent,<sup>2</sup>  
Peter N. Devreotes,<sup>3</sup> and Cornelis J. Weijer<sup>1,4</sup>

<sup>1</sup>School of Life Science  
University of Dundee  
Wellcome Trust Biocentre  
Dow Street  
Dundee, DD1 5EH  
United Kingdom

<sup>2</sup>Laboratory of Cellular and Molecular Biology  
National Cancer Institute  
National Institutes of Health  
37 Convent Drive  
Bethesda, Maryland 20892-4255

<sup>3</sup>Department of Biological Chemistry  
Johns Hopkins University  
School of Medicine  
725 North Wolfe Street  
Baltimore, Maryland 21205

## Summary

**Background:** Starving amoebae of *Dictyostelium discoideum* communicate by relaying extracellular cAMP signals, which direct chemotactic movement, resulting in the aggregation of thousands of cells into multicellular aggregates. Both cAMP relay and chemotaxis require the activation of PI3 kinase signaling. The spatiotemporal dynamics of PI3 kinase signaling can be followed in individual cells via the cAMP-induced membrane recruitment of a GFP-tagged PH domain-containing protein, CRAC, which is required for the activation of adenylyl cyclase.

**Results:** We show that polarized periodic CRAC-GFP translocation occurs during the aggregation and mound stages of development in response to periodic cAMP signals. The duration of CRAC translocation to the membrane is determined by the duration of the rising phase of the cAMP signal. The system shows rapid adaptation and responds to the rate of change of the extracellular cAMP concentration. When the cells are in close contact, it takes 10 s for the signal to propagate from one cell to the next. In slugs, all cells show a permanent polarized PI3 kinase signaling in their leading edge, which is dependent on cell-cell contact.

**Conclusions:** Measuring the redistribution of GFP-tagged CRAC has enabled us to study the dynamics of PI3 kinase-mediated cell-cell communication at the individual cell level in the multicellular stages of *Dictyostelium* development. This approach should also be useful to study the interactions between cell-cell signaling, cell polarization, and movement in the development of other organisms.

## Introduction

Chemotactic cell movement plays an important part in many biological processes ranging from the movement

of leukocytes toward pathogens, wound closure, formation of metastasized tumors, and angiogenesis to the extensive tissue rearrangements occurring in embryonic development [1]. In order to understand these processes, it will be necessary to analyze the interplay between the signals controlling cell behavior and their detection and transduction by responding cells to result in cell movement, tissue rearrangements and morphogenesis. Significant advances in our ability to visualize the dynamics of key cellular processes involved in chemotactic signal transduction have been made through the use of time-lapse imaging of the translocation of GFP-tagged signaling proteins [2–4], and it now becomes possible to study these events in the context of tissues and even whole organisms.

The signal transduction pathways underlying signal detection, cell polarization, and chemotaxis are widely investigated in leucocytes and *Dictyostelium discoideum* amoebae and have been shown to involve localized activation of PI3 kinase signaling in the leading edge of the cell [2, 3, 5, 6].

*Dictyostelium* amoebae undergo a starvation-induced multicellular developmental cycle, which involves the chemotactic aggregation of hundreds to thousands of cells into a multicellular aggregate that continues to develop into a fruiting body. The aggregation process is governed by chemotaxis toward waves of cAMP, periodically initiated from the aggregation center and relayed outward by surrounding cells, resulting in the outward propagation of cAMP waves. These waves direct the inward movement of the cells toward the aggregation center and can be detected as optical density (OD) waves. We have observed these OD waves during all stages of development, suggesting that chemotaxis in response to cAMP waves is the principle that controls cell movement during all stages of development [7, 8].

cAMP is detected via serpentine cAMP receptors, and binding of cAMP to a serpentine cAMP receptor results in both the activation of the cAMP relay response and chemotaxis. Receptor-mediated activation of PI3 kinase, resulting in the production of phosphatidylinositols, especially PI [3, 4]P<sub>2</sub> (PIP<sub>2</sub>) and PI [3, 4, 5]P<sub>3</sub> (PIP<sub>3</sub>), is a key step in the cAMP relay response. Activation of the PI3 kinase directs the transient localization of the Pleckstrin Homology (PH) domain-containing protein CRAC (cytosolic regulator of adenylyl cyclase) to the membrane, an essential step in the activation of the aggregation-stage adenylyl cyclase (ACA) [9, 10]. cAMP-mediated PI3 kinase activation is also an essential step in chemotaxis, since it is necessary for localized actin polymerization and the control of myosin phosphorylation via the recruitment of another PH domain-containing protein, Akt/PKB, to the membrane. Akt/PKB is involved in the suppression of lateral pseudopodia, via the activation of PAK, which results in the inhibition of myosin-kinase and myosin thick filament disassembly in the rear of the cell [4, 11–13].

Stimulation of aggregation-stage cells with a uniform stimulus of cAMP results in the rapid, uniform, transient

<sup>4</sup>Correspondence: c.j.weijer@dundee.ac.uk

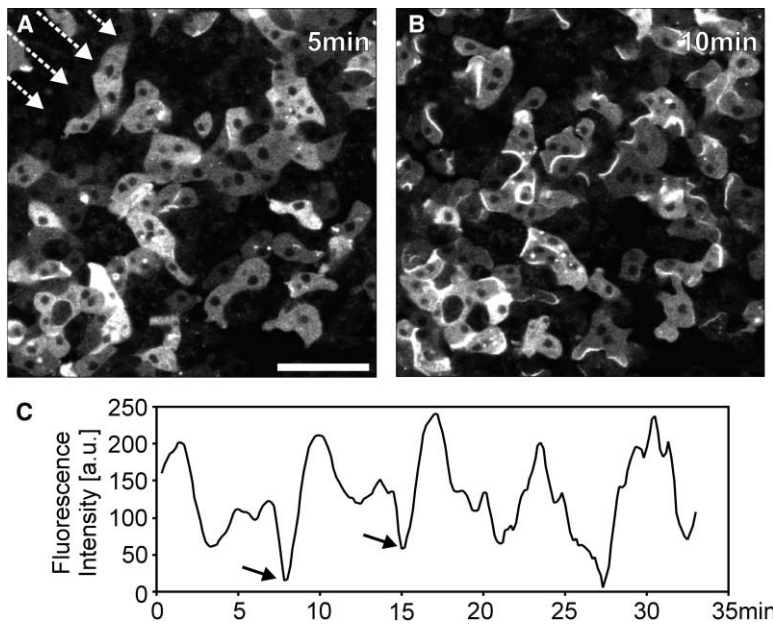


Figure 1. Periodic CRAC-GFP Membrane Translocation during Early Aggregation

(A) A fluorescence image showing a monolayer of cells with cytoplasmic CRAC-GFP, 4 hr after the onset of starvation. The arrows indicate the direction of wave propagation.

(B) Five minutes later, a cAMP wave has passed through the population, inducing CRAC-GFP membrane localization.

(C) A graph showing the periodic changes in fluorescence intensity as several waves travel through the cell population. The arrows mark the passing of the slightly darker wave fronts. Due to focus drift, the intensity data were corrected by subtracting the values of a calculated fitted curve from the original data. The scale bar represents 30  $\mu\text{m}$ .

translocation of PH domain proteins CRAC and Akt/PKB to the membrane. However, cells migrating in a gradient of cAMP show a localized translocation of CRAC and Akt/PKB to the leading edge of the cell. These proteins can therefore be used to monitor the polarization of aggregation-stage cells in response to an external cAMP gradient.

Here, we measure the translocation of GFP-tagged CRAC to investigate the dynamics of cell-cell signaling and cell polarization in the multicellular stages of *Dictyostelium* development. Cells show strongly polarized CRAC binding at their leading edge during all stages of development. During aggregation and in the mound stage, cAMP-dependent PIP3 signaling shows rapid adaptation, which ensures that the duration of CRAC binding to the membrane is determined by the duration of the rising phase of the cAMP signal in vivo. In the slug stages, the cells show a permanent activation of PIP3 signaling at their leading edges. This polarization of PIP3 signaling in the direction of cell migration is cell contact dependent and does not adapt in response to cAMP stimulation anymore, suggesting a dramatic change in the mechanism of cell polarization.

## Results

### Periodic CRAC-GFP Membrane Translocation during Early Aggregation

Several hours after the onset of starvation, *Dictyostelium* cells start to initiate and propagate cAMP waves that spread rapidly through the cell population with velocities of up to several hundred micrometers per minute [14, 15]. Figure 1A shows a monolayer of cells with predominantly cytoplasmic CRAC-GFP, although some cells still contain brightly labeled macropinosomes. A few minutes later, a cAMP wave has passed through the population, resulting in the translocation of CRAC-GFP to the plasma membrane (Figure 1B). At this stage, the CRAC-GFP membrane localization is very heterogeneous; in

some cells it is bound to one side of the cell, while, in others, it is almost uniformly spread over the entire plasma membrane. There is some movement toward the source of the cAMP waves, but random movement prevails. Although it proved difficult to visualize the wave fronts that propagated at about 300  $\mu\text{m}/\text{min}$ , it was possible to capture the response of the cell population as a whole by measuring the average fluorescence intensity over the entire image following background subtraction (see the Experimental Procedures). The graph in Figure 1C shows the periodic changes as several waves pass through the population (periodicity:  $7.4 \pm 1.1$  min). The peaks correspond to images in which a majority of cells show membrane localization of CRAC-GFP. The arrows in the graph (Figure 1C) mark the passing of the slightly darker wave fronts, which result from a decrease in cytoplasmic fluorescence as CRAC-GFP starts to translocate to the plasma membrane. The translocation of CRAC-GFP can be completely inhibited by the PI3 kinase inhibitor LY294002 (20  $\mu\text{M}$ ), 50  $\mu\text{M}$  of the specific cAMP receptor cAR1 inhibitor IPA (isopropylidene adenosine) [16], or by 5 mM caffeine, a well-known inhibitor of cAMP relay [14, 17], showing that cAMP is the signal that causes activation of PI3 kinase and PIP3 production. We have determined that CRAC-GFP binds to PIP3 in the membrane using lipid blot overlay assays to determine the lipid binding specificity of CRAC and a range of GFP-tagged PH domains to determine the active species in the membrane (D.D. et al., unpublished data).

As fixed signaling centers appear, the cells start to move chemotactically toward these centers. Figure 2A shows the wave-like spread of CRAC-GFP membrane translocation in cells of an aggregation stream. The CRAC translocation is now restricted to the leading edge of the cells, as described previously for chemotactically moving cells in vitro [9]. The cells are in close contact and are moving toward a signaling center on the left-hand side. The arrow tips mark the position of the wave front, as identified by the position of cells with new

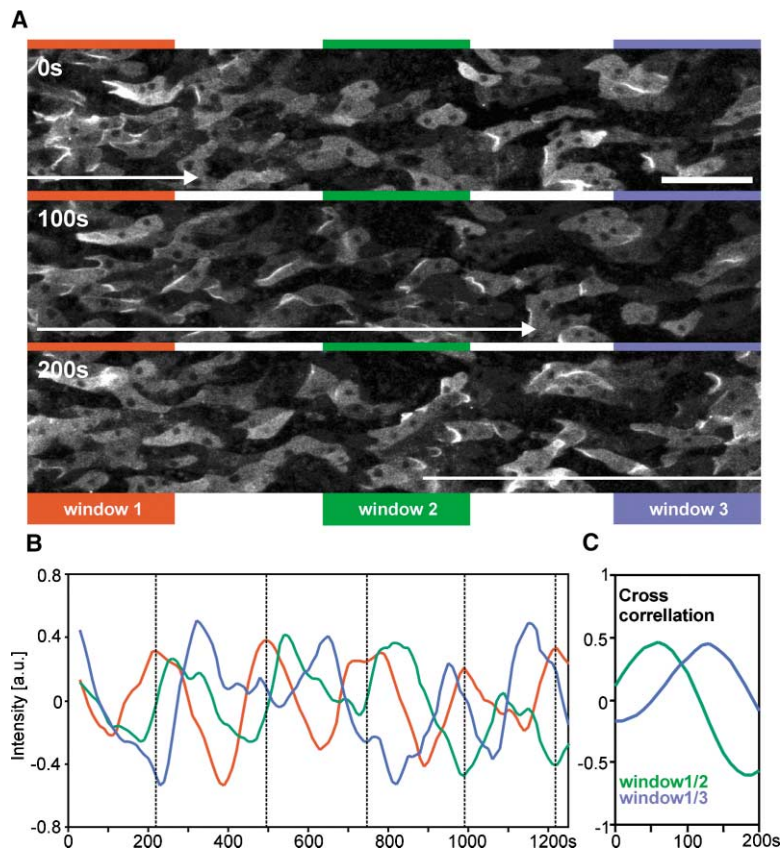


Figure 2. CRAC-GFP Translocation in Aggregation Streams

(A) A sequence of images showing the spread of CRAC-GFP membrane translocation along an aggregation stream ( $t = 5.5$  hr). The arrow tips mark the position of the wave front identified by the cells with membrane-bound CRAC-GFP; the length of the arrows indicates the width of the wave. The wave propagates from left to right. A few cells on the right-hand side of the “0 s” image still show membrane-bound CRAC-GFP, as they haven’t recovered yet from the previous excitation wave.

(B) A graph showing the normalized changes of fluorescence intensities recorded in the three different areas (“window1–3”), as indicated and color coded in (A). The waves are first detected in “window1”, then with a delay in “window2”, and finally in “window3”.

(C) Cross-correlation between the different curves in (B). Green curve: cross-correlation between the curves derived from window1 and window2; blue curve: cross-correlation between the curves derived from window1 and window3. The scale bar represents  $30 \mu\text{m}$ .

CRAC-GFP membrane localization. Within about 3 min, the wave has crossed the field of view, which can be followed in real time as one cell after the other shows the CRAC-GFP translocation. The membrane localization of CRAC is only transient, and the length of the arrows indicates the width of the wave front where CRAC-GFP is membrane bound. In order to quantify the wave propagation speed and periodicity, we measured the average intensity in three 200-pixel-wide windows following background subtraction (see the Experimental Procedures; Figure 2A). When plotted against time, a phase shift between the curves can be observed (Figure 2B), which is due to the propagation of the extracellular cAMP signal that causes CRAC translocation. The dashed lines in the graph mark the intensity peaks that were measured in “window1”; the peaks of the other two curves are shifted toward the right. The exact phase shift can be determined by calculating the cross-correlation between these curves (Figure 2C; phase shift: window1/2, 60 s; window1/3, 130 s). Together with the distance between the measuring windows, the wave propagation speed was calculated to be  $\sim 90 \mu\text{m}/\text{min}$ , which matched values that were derived previously from the analysis of optical density waves [14]. The wave period was  $4.25 \pm 0.48$  min ( $n = 6$ ), and the cells seemed to respond to each wave as shown in Figure 3. The cell goes through six cycles of CRAC-GFP membrane translocation, followed by adaptation and subsequent dissociation of CRAC-GFP from the membrane. This is also accompanied by periodic cell shape changes. We often observed that the leading edge appeared to be

V-shaped, which is particularly obvious when CRAC-GFP is bound to the membrane (Figure 3). The cells almost seem to engulf the posterior part of the cells in front. It can be seen how the cAMP signal is propagated from a cell to its immediate neighbors (Figure 4). In this sequence, one cell after the other exhibits CRAC membrane localization (indicated by stars), with a delay of about 10 s.

#### Wave Propagation and CRAC-GFP Translocation in Mounds

The aggregating cells finally form mounds in which cell behavior is still coordinated by propagating waves of cAMP. We observed waves of CRAC-GFP translocation in the shape of single-, double-, or multiarmed spiral waves (data not shown), which were very similar to previously described wave patterns [18]. In the example of Figure 5, the clockwise cell movement was controlled by a single arm spiral wave that rotated counterclockwise.

A single cell was tracked over 10 min as it rotated around the mound, showing periodic CRAC-GFP translocation to the leading edge (Figure 5A, images marked with an asterisk), which was quantified by measuring the average fluorescence intensity (Figure 5B). Following image subtraction to enhance the visibility of the propagated wave, we were also able to detect the passing of the slightly darker wave front by computing the local brightness at the position of the cell. The graph in Figure 5B shows the close correlation between the optical density wave and the recruitment of CRAC-GFP to the leading edge; whenever the wave front reaches the cell,

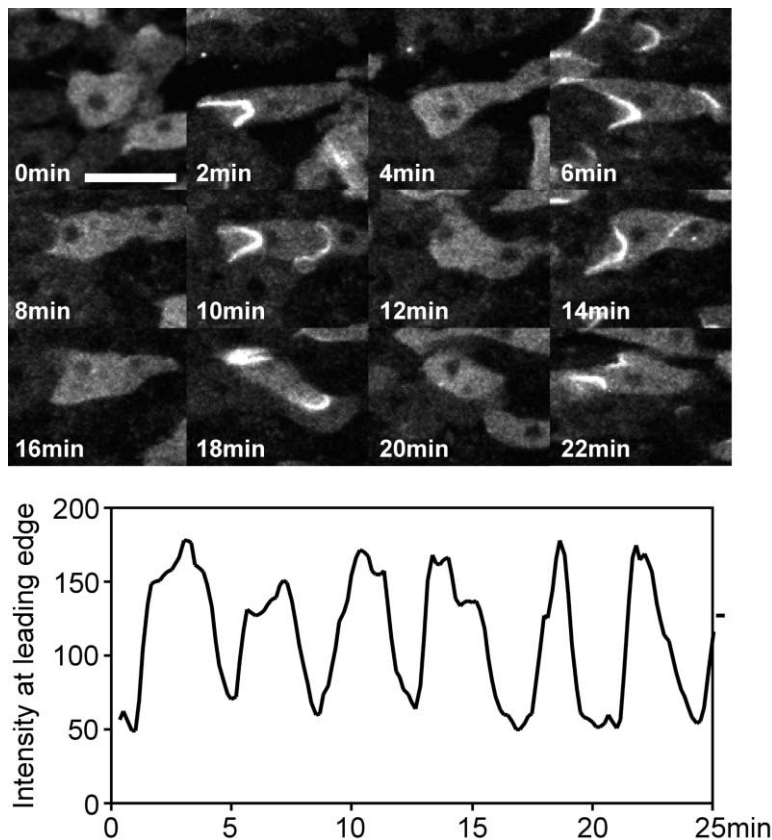


Figure 3. Periodic CRAC-GFP Translocation to the Leading Edge in Aggregation Streams  
Snapshots of a single cell, which was tracked in the aggregation stream shown in Figure 2. CRAC-GFP translocates periodically to the leading edge. The fluorescence intensity measured in a  $10 \times 10$  pixel window at the leading edge is shown in the lower panel. The scale bar represents  $15 \mu\text{m}$ .

CRAC-GFP translocates to the membrane. The wave propagation speed was measured to be about  $50\text{--}60 \mu\text{m}/\text{min}$ , in agreement with previous findings. The period of CRAC-GFP membrane translocation was very short ( $97 \pm 21 \text{ s}$ ; 12 cells in 4 mounds), indicating that cells become readily excitable again once they have adapted. Periodic CRAC translocation can be completely inhibited by  $100 \mu\text{M}$  cAMP or its nonhydrolyzable cAMP analog Sp-cAMPS.

#### Membrane Binding of CRAC-GFP Changes during Development

Although aggregating cells always respond to the extracellular signal waves with a transient membrane translocation of CRAC-GFP, the duration of membrane binding changes drastically during development. During the early phases of aggregation when dark-field waves are present, CRAC-GFP remains at the membrane for up to 2.5 min (Figure 6A). This decreases to  $\sim 70\text{--}100 \text{ s}$  in streams and then further down to  $49 \pm 18 \text{ s}$  ( $n = 8$  mounds) at the mound stage.

To test whether this change in membrane binding is a cell autonomous effect, we took developing cells from agar plates at different stages and stimulated them with micromolar cAMP pulses, while recording the behavior of cells aggregating on the plates on another microscope at the same time (Figure 6A). The cAMP-induced membrane translocation always lasted about  $\sim 8\text{--}10 \text{ s}$ , which was very different from the *in vivo* data. Figure 6B shows the typical response of an aggregation-competent cell that has been stimulated with a cAMP pulse.

Translocation peaks within 5–6 s, followed by rapid dissociation. The translocation to the membrane appears to be slightly slower in developing cells *in vivo*, but membrane binding is extended quite considerably (Figure 6B). However, we cannot determine the exact time point when the cells start sensing the cAMP signal *in vivo*, which makes comparisons difficult. We also studied cells that were aggregating when submerged under buffer. The coordinated periodic CRAC-GFP translocation in those cell populations indicated autonomous cAMP signaling. When these cells were pulsed with cAMP several minutes after the last endogenous cAMP wave had passed, membrane binding of CRAC-GFP lasted, again, only  $\sim 10 \text{ s}$  (data not shown), suggesting that the observed developmental change in CRAC-GFP membrane association is not an effect that is dependent on changes in the intracellular signal transduction mechanism, but reflects changes in the kinetics of the cAMP signal perceived by the cells at different stages of development. During aggregation, the rising flank of the cAMP lasts several minutes [15, 19].

In order to directly show that the duration of CRAC-GFP membrane translocation is determined by the duration of the cAMP rise, aggregation-competent cells were mounted in a perfusion chamber, where they were exposed to an increasing temporal cAMP gradient ( $0\text{--}10^{-6} \text{ M}$  over 5 min), simulating the rising phase of a natural cAMP wave. Under these conditions, with a slowly rising cAMP concentration, CRAC-GFP translocates to the plasma membrane but then remains there much longer, comparable to cells in aggregation streams or mounds

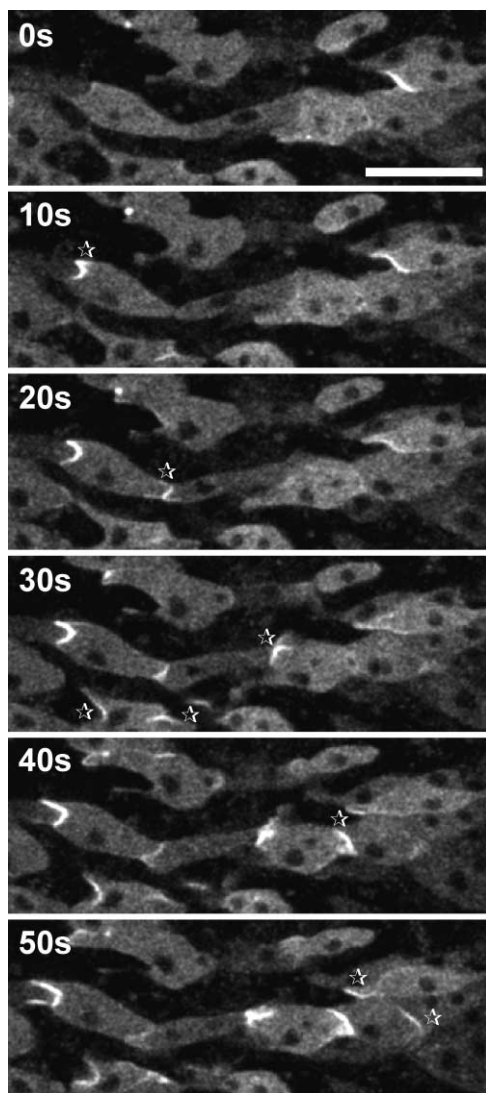


**Figure 4. Propagation of CRAC-GFP Membrane Translocation**  
One cell after the other shows membrane localization of CRAC-GFP at the leading edge in an aggregation stream. Stars mark the first appearance of membrane-bound CRAC-GFP. The scale bar represents 20  $\mu\text{m}$ .

(Figures 6A and 6C). The gray bar in Figure 6A summarizes the results of 25 cells from three independent experiments that were performed under similar conditions. We conclude from these data that the shape of the cAMP signal is an important and probably the determining factor influencing the duration of CRAC-GFP membrane binding during aggregation *in vivo*.

#### Slug Cells Show Constant Polarized Membrane Localization of CRAC-PH-GFP

Since we have recently observed propagating OD waves in slugs, we tried to establish whether this is mirrored by periodic CRAC-GFP membrane translocation in slug cells. Although CRAC-GFP was expressed under the constitutively active *actin15* promoter, almost no fluorescent cells were detectable at the slug stage (data

not shown), suggesting a downregulation of CRAC-GFP expression during later development. This was overcome by expressing only the N-terminal PH domain of CRAC fused to GFP, resulting in a fusion protein with basically identical properties to CRAC-GFP in terms of lipid binding specificities, membrane translocation, and binding kinetics (data not shown). CRAC-PH-GFP protein expression was observed in slugs when it was expressed under the control of the *actin15* promoter; however, it was only detected in cells in the prestalk O region of the slug and in scattered anterior-like cells in the prespore zone (Figure 7A). Membrane localization was the highest at the anterior leading edge of the cells but was often more widespread along the plasma membrane compared to aggregating cells (Figure 7B).

Although individual slug cells were tracked for up to 40 min, we could not detect clear periodic changes in CRAC-PH-GFP membrane localization (36 tracked cells from 22 slugs). In 22 cells, the fluorescent probe appeared to be constantly membrane bound, while, in 11 cells, the membrane association was interrupted by short phases lacking membrane binding ( $59 \pm 48$  s;  $n = 26$ ; 5 cells), without any clear periodicity. As movement and shape changes of the tracked cells were a major obstacle in the analysis of CRAC-GFP localization, we decided to block cell motility without interrupting cell-cell signaling by using LatrunculinA (LatrA), which binds to monomeric G-actin in a 1:1 complex and disrupts actin microfilaments [9]. In initial tests, mounds were developed on dialysis membrane and were transferred onto agar containing 2–5  $\mu\text{M}$  LatrA. Cells rounded up and movement ceased within minutes, but signaling still occurred, as was evident from propagated waves of CRAC-GFP membrane translocation (data not shown). In slugs, cell movement stopped rapidly as well, but CRAC-PH-GFP remained constantly membrane bound and also, in many cases, seemed to keep on showing a distinct polarization (Figure 7C).

We investigated CRAC-PH-GFP localization in mechanically dissociated slug cells. Isolated slug cells hardly ever showed membrane-bound CRAC-PH-GFP (1 out of 34 cells), while, on the other hand, cells that seemed to be in direct contact with other cells in small groups often exhibited membrane localization at the site of cell-cell contact (59 out of 142 cells). In order to test whether this membrane localization was still dependent on cAMP signaling, we incubated slugs and small groups of slug cells in millimolar cAMP concentrations. Although the cAMP rapidly resulted in a cessation of directed cell movement, we did not find any decrease of the CRAC-GFP membrane localization, suggesting that the response either did not show any adaptation to cAMP or was not mediated via cAMP (Figures 7C and 7D). Furthermore, we noted that many of the cells even stayed polarized in the presence of high levels of cAMP (see cells with an asterisk in Figures 7C and 7D). To investigate whether cAMP could still polarize slug cells, we performed chemotaxis experiments with single cells from mechanically dissociated slugs. In 13 experiments, only a small number of cells moved toward the cAMP microelectrode, none of which showed any clear membrane localization of CRAC-GFP. We have established that isolated slug cells cannot move readily on a glass

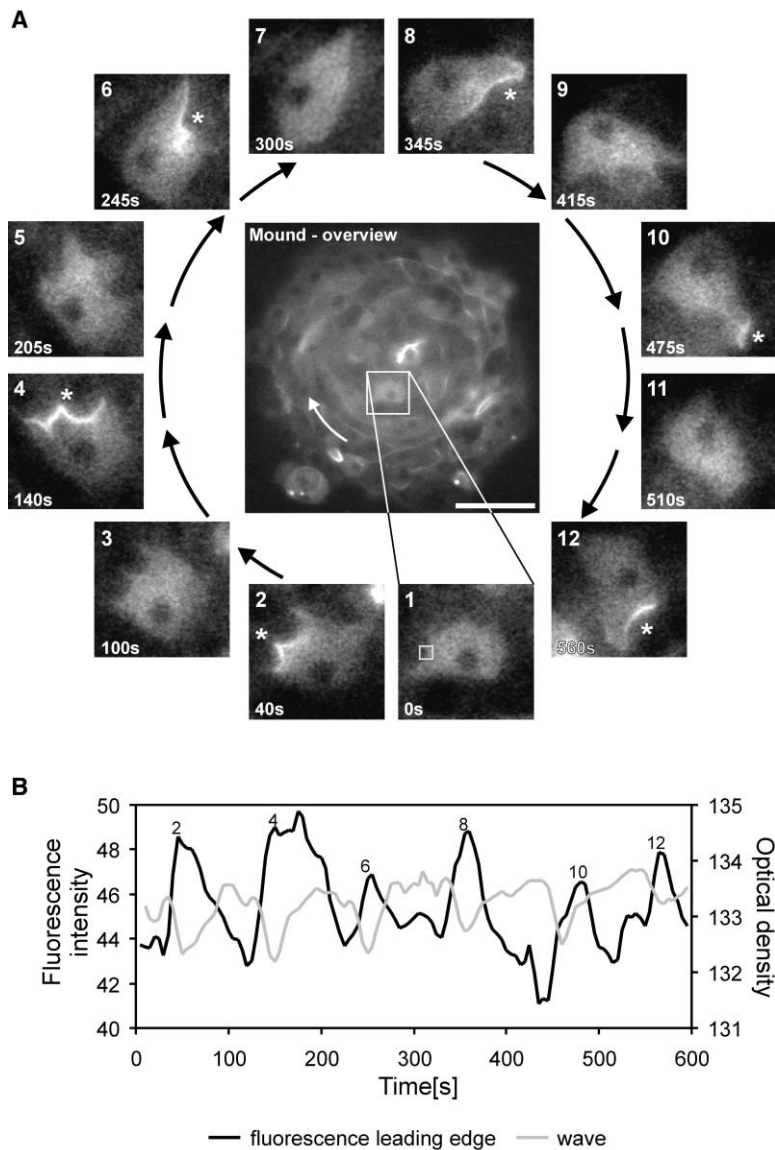


Figure 5. CRAC-GFP Localization and Wave Propagation in Mounds

(A) One cell was followed as it moved counterclockwise around the mound shown in the center; a single-arm spiral wave was propagating in the opposite direction. Images with membrane-bound CRAC-GFP are marked by asterisks.

(B) A correlation between fluorescence intensity at the leading edge and wave propagation. The fluorescence was measured in a  $10 \times 10$  pixel window as shown in (A), image 1. The intensity of the dark-field wave was measured at the position of the cell in a  $100 \times 100$  window following image subtraction. The wave appears as a dark wave front, hence the periodic drop in optical density, which coincides with CRAC membrane localization. The scale bar represents  $25 \mu\text{m}$ .

surface; in the slug stage, they become dependent on cell-cell and cell matrix interactions to move. We therefore examined cells that had just been left behind in the slime trail, a substrate on which they can move and which is left behind during migration at the posterior end of the slug. We found a clear response to cAMP gradients, with membrane localization of CRAC-PH-GFP at the side of the cell facing the higher cAMP concentration, showing that these cells in contact with a suitable matrix can still polarize in response to cAMP signals (data not shown).

When we expressed CRAC-GFP from either a prestalk-specific *ecmA* promoter or a prespore-specific *PspA* promoter, expression was observed in all prestalk and prespore cells. Prestalk cells in the tip often appeared flattened, with their long axis perpendicular to the long axis of the slug, but, nevertheless, with strong localization of CRAC-PH-GFP toward the anterior side of the cell (Figures 7F and 7G, arrows). Prespore cells, the spore precursor cells in the posterior part of the

slug, looked very similar, with a stronger membrane localization at the cell anterior. The schematic drawing in Figure 7I summarizes the observed patterns of CRAC-PH-GFP membrane localization. In conclusion, we find that, in intact slugs, PI3 kinase signaling is continuously polarized in the direction of cell migration, but it seems likely that this is now mediated via a cell-cell contact-dependent mechanism that still could be modulated by cAMP signaling.

## Discussion

### PIP3-Mediated Signaling in the Aggregation and Mound Stages

We have studied PIP3-mediated cell-cell signaling during the entire life cycle of *Dictyostelium* using the membrane translocation of the PIP3 binding protein CRAC-GFP. During all phases of development, cells showed polarized PIP3 signaling. The polarity of PIP3 signaling always coincided with the direction of movement in that

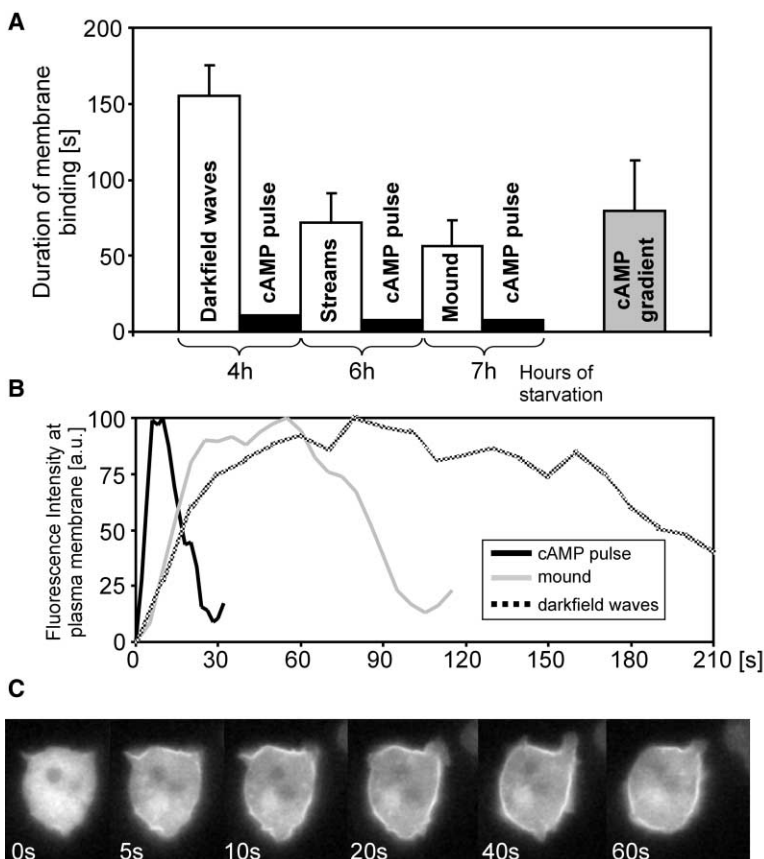


Figure 6. The Duration of CRAC Membrane Binding Changes during Development

(A) The duration of membrane binding was measured at the indicated time points for cells aggregating on agar plates (df waves, streams, and mounds; white bars), while, at the same time, cells were taken from the plates and were pulsed with micromolar concentrations of cAMP *in vitro* (black bars). The gray bar represents cells in a perfusion chamber that were exposed to a cAMP gradient. The mean values and standard deviations are shown.

(B) A comparison of the kinetics of CRAC-GFP membrane binding. The curves were normalized to correct for different fluorescence intensities. The typical cAMP-induced response in an aggregation-competent cell is compared to the membrane localization of cells in mounds and during early aggregation when dark-field waves are present. The cAMP pulse induces rapid but short-lived membrane association.

(C) Longer lasting CRAC-GFP membrane binding in a cell exposed to a slowly rising temporal cAMP gradient. The cAMP concentration was slowly increased from 0 to  $10^{-6}$  M cAMP in a linear fashion over a period of 4 min using a gradient mixer.

the highest PIP3 levels were detected at the leading edge of the cell. The dynamics of CRAC localization varied, however, with the different developmental stages. During the aggregation and mound stages, the cells showed a periodic CRAC translocation to their leading edge. cAMP pulsing experiments with single aggregation-competent cells had shown that the translocation of CRAC shows rapid adaptation [9]. We have now shown that the kinetics of this adaptation response is essentially unchanged *in vitro* in aggregation- and mound-stage cells ( $\sim 10$  s; Figures 6A and 6B). This contrasts strongly with the much longer membrane association of CRAC-GFP observed *in vivo*. The duration of CRAC translocation changed during development. The longest association ( $\sim 3$  min) was found in the early aggregation stages, and it then became shorter during the development to the mound stage ( $\sim 1$  min, Figures 6A and 6B), matching previous measurements on the dynamics of optical density waves that also showed a significant decrease in period during early development [18, 20, 21]. During early aggregation, the period of the OD waves is around 6 min, and this decreases to around 2 min in the mound stage [21]. Therefore, the duration of CRAC membrane binding *in vivo* is half the period of the optical density waves. We have shown previously that the OD waves reflect changes in coordinated cell movement in streams and mound and that they are dependent on the periodic activation of the aggregation-stage adenylyl cyclase ACA, by the use of a temperature-sensitive ACA mutant [22]. Therefore, the duration of

CRAC translocation is associated with the rising phase of the cAMP, which is half the period of the OD waves. Furthermore, CRAC translocation is completely inhibited by saturating levels of cAMP, which results in adaptation of the PI3 kinase pathway and an associated adaptation of directed chemotactic movement. Incubation of aggregation-stage cells with the cAR1 receptor inhibitor IPA also results in a block of CRAC translocation and chemotactic movement, showing that the *in vivo* signal that gives rise to periodic PIP3 production is a periodic cAMP signal. Therefore, the spatiotemporal dynamics of CRAC translocation observed at these stages of development reflect the spreading of the cAMP signal as detected at the individual cell level.

#### During Early Development, the PIP3 Response Shows Fast Adaptation

We have shown that CRAC-GFP binds the membrane transiently during a step up in concentration, indicative of rapid adaptation, but continuously, during the rising phase of a temporal cAMP gradient (Figure 6C). It appeared that the CRAC-GFP intensity at the membrane, and therefore the PIP3 level, was constant during the course of the temporal gradient. This implies that the rate of change of the cAMP concentration is proportional to the PIP3 concentration in the membrane. PI3 kinase activation is mediated via  $G\beta\gamma$  [23, 24], but it has also been shown that adaptation occurs at a point in the pathway beyond the activation of the G protein, since continuous cAMP stimulation results in continuous acti-

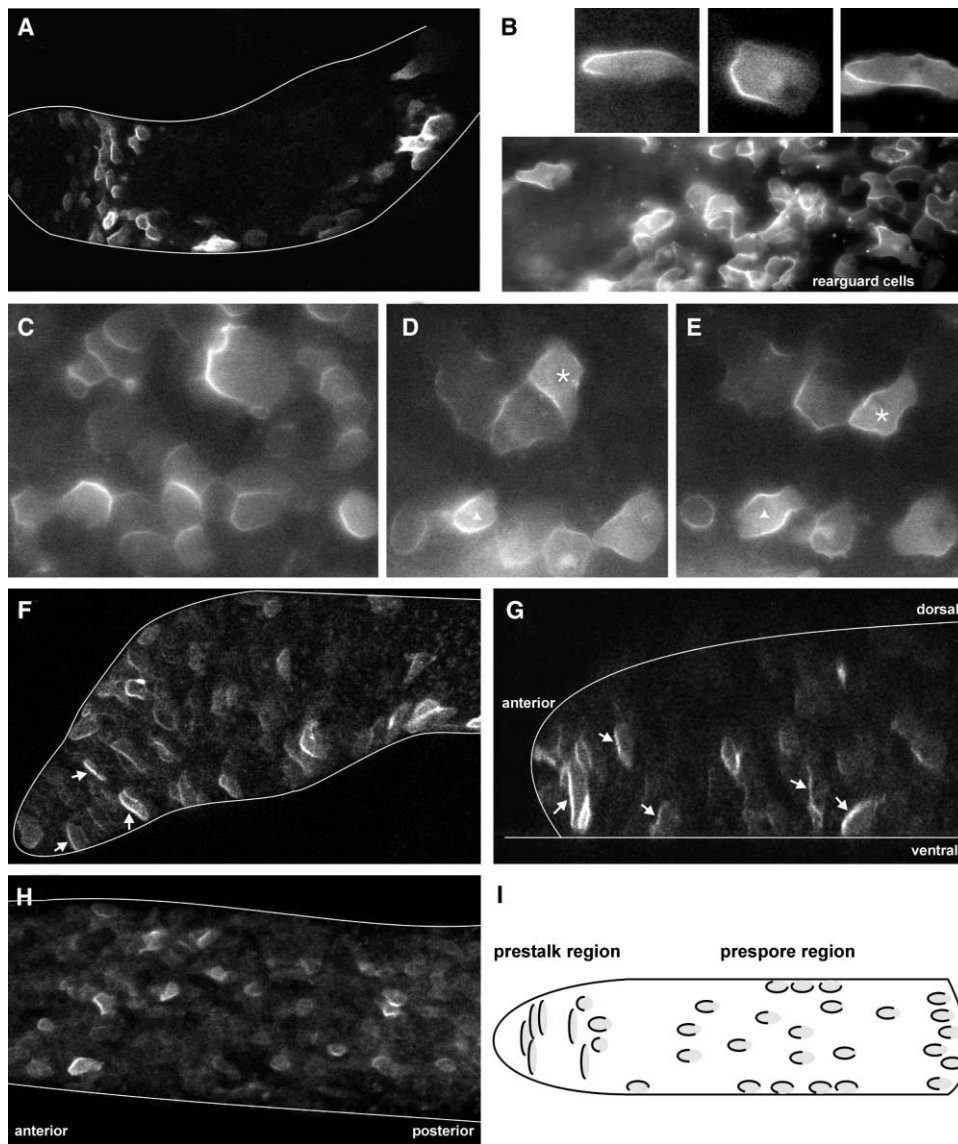


Figure 7. Membrane Localization of CRAC-PH-GFP in Slugs

- (A) The slug of a cell line expressing the CRAC-PH-GFP under the control of the constitutive *actin15* promoter. Brightly fluorescent cells are only found in the *ecmO* zone of the slug tip and in anterior-like cells in the back of the slug.
- (B) Membrane localization in cells of these slugs expressing *actin15::CRAC-PH-GFP*. Three cells are shown with localized binding at the anterior side of the cell. The figure underneath shows cells in the back of a slug.
- (C) A view of the back of a slug showing polarized CRAC-PH-GFP binding 1.5 hr after the transfer onto agar containing 2  $\mu$ M Latrunculin A. Slug movement had stopped completely by this stage.
- (D) A slug, 1 hr after transfer on agar containing 1 mM cAMP; slug movement had stopped.
- (E) The same part of the slug that is shown in (D) after a further 10 min of incubation on 1 mM cAMP. The same two cells are marked (asterisk, arrowhead) in (C) and (D) to show that they have not moved appreciably during the time of the experiment and that they continue to show polarized CRAC-GFP binding in the presence of cAMP.
- (F) Confocal *xy* section of a slug expressing CRAC-PH-GFP under the control of the prestalk-specific *ecmA* promoter. CRAC-PH-GFP membrane binding is clearly polarized in prestalk cells in the slug tip (arrows).
- (G) Confocal *xz* section through the midline of a slug expressing CRAC-PH-GFP under the control of the *ecmA* promoter showing membrane binding at the anterior side of the cells.
- (H) The prespore region of a slug migrating to the left showing CRAC-PH-GFP localization driven by the prespore-specific promoter *PSA*.
- (I) A schematic diagram showing the membrane localization (black lines) of cells (gray) in different parts of the slug.

vation of the receptor-coupled G protein  $G\alpha 2\beta\gamma$  [25]. It is not exactly known how many steps there are between the formation of free  $G\beta\gamma$  and PIP3 production and destruction and where adaptation occurs, but it will be a

challenge to identify the underlying molecular mechanism. The rapid adaptation of the CRAC PH domain localization response shown here ensures that the cells can react rapidly to changes in signal direction. It is

likely that this ability will be important during the early stages of development, i.e., it could facilitate the formation of aggregation streams and the movement of cells around obstacles.

### PI3 Kinase Signaling in Slugs

In slugs, the cells showed a continuous, polarized membrane association of CRAC in the leading edge of the cell, indicating that PI3 kinase signaling was activated continuously in a polarized fashion. This continuous polarization implies that the cells either experience a continuous activating signal or that the dynamics of the internal transduction mechanism, rate of PIP3 synthesis, and/or breakdown have changed. Furthermore, the question remains whether the stimulatory signal in slugs is still cAMP or whether the PI3 kinase signaling pathway is now coupled to another signaling pathway. Dissociated slug cells showed no sign of CRAC membrane translocation, but cells in small groups showed CRAC-PH-GFP localization at the membrane in areas of cell-cell contact. However, CRAC-PH-GFP membrane localization was not inhibited by the presence of millimolar cAMP concentrations either in intact slugs or in small groups of cells. Even more surprising was the finding that, although the cells in the slug did not show any significant directed movement anymore in the presence of millimolar cAMP concentrations, the cells continued to show polarized PIP3 localization in their membranes facing the tip (Figures 7D and 7E). We found that PIP3 disappeared rapidly upon dissociation of slug tissue, and we did not succeed in inducing PIP3 with cAMP in these dissociated cells. These experiments showed that there was no adaptation of the CRAC PH domain membrane localization in response to cAMP anymore, as was found in the earlier stages of development, and that PIP3 signaling is now mainly responsive to another signaling pathway. We consider it most likely that, in the slug stage, polarized PI3 kinase signaling is linked to a cell-cell contact-mediated signaling pathway.

The polarization of PIP3 production does not seem to depend on the actin cytoskeleton, since PIP3 localization was found to persist in slugs treated with Latrunculin A (Figure 7C). We also observed that polarization of PIP3 signaling of cells located in the back of slugs persisted, even when the tip was surgically removed, making it unlikely that the polarization signal is a long range-signal coming from the tip, but more likely that it depends on local cell-cell interactions. This observation has to be reconciled with the well-documented function of the tip as the organizer of cell movement in the slug [20, 26] and the fact that propagating optical density waves can be observed in slugs of many *Dictyostelium* strains. These waves reflect periodic cell movement in response to a signal initiated in the tip of the slug [20]. Furthermore, we suggested that this signal was cAMP, since all the components necessary to produce cAMP oscillation enzymes such as ACA, CRAC G $\alpha$ 2, and PDE are expressed in the prestalk and anterior-like cells [27, 28]. It is, however, also known that cells that lack the aggregation-stage adenylyl cyclase ACA can still form slugs and fruiting bodies when they overexpress the catalytic subunit of the cyclic AMP-dependent protein

kinase [29]. This indicates that, under some circumstances, slugs can move using a different mechanism, such as contact following, which will still require the cells to be polarized and in which the observed polarized PIP3 signaling may play a role.

These findings open up many new questions; what is the signaling mechanism of the contact-dependent polarization of PIP3 signaling in slugs? What is the biological role of continuous contact-dependent PIP3 signaling polarization of slug cells? Does this contact-dependent polarization imply the existence of a contact-following mechanism? How does the PIP3 signaling system interact with the cAMP signaling system that has been implicated to direct the chemotactic movement of cells in slugs [20, 30, 31]? All of these questions have to await further investigation.

### Experimental Procedures

#### Strains and Cell Culture

The cell line expressing the CRAC-GFP fusion protein was the same as described previously [9]. We also created constructs with the N-terminal PH domain of CRAC fused to GFP. A 700-bp fragment containing the PH domain was amplified from vector pRH123 by PCR using primers with HindIII and BamHI sites. The PCR product was cloned into the GFP expression vector pb15rsGFP, which gives constitutive expression under the control of the actin15 promoter. For cell type-specific expression, the PH domain-GFP fragment was excised using XhoI and BamHI and was inserted into BglII and XhoI cut vectors containing prestalk- and prespore-specific promoters. Ax2 cells were electroporated with the different plasmids, and stable transformants were selected in 10  $\mu$ g/ml G418. The wild-type strains NC4 and NP377 were grown on SB agar plates containing *Klebsiella aerogenes* [32].

To induce development, cells were washed once in KK2 phosphate buffer (20 mM KH<sub>2</sub>PO<sub>4</sub>/K<sub>2</sub>HPO<sub>4</sub> [pH 6.8]), plated on 1% KK2 agar (Difco, Bacto-Agar) at a density of  $8 \times 10^5$  cells/cm<sup>2</sup>, and incubated at 22°C [20]. Slugs were prepared as described [33]. For cell tracking experiments, slugs were made from either 100% CRAC-PH-GFP cells or chimeras of 5% CRAC-PH-GFP with 95% NC4 or NP377 cells.

#### Live Cell Microscopy

The agar plates with the cells were incubated until they had reached the required developmental stage. In order to study CRAC-GFP membrane translocation up to the mound stage, small pieces of agar ( $\sim 1$  cm<sup>2</sup>) were cut out and carefully placed upside down on a glass coverslip mounted in an Attofluor cell chamber (Molecular Probes) so that the cells were slightly squashed between the agar and coverslip. This had no detrimental effect on cell behavior for up to several hours and gave the best optical conditions. To prevent desiccation, the agar was covered with silicon oil (Dow Corning 200/20 cs). Slugs were treated similarly, but sometimes spacers between the agar and coverslip were used to avoid extensive squashing.

For most studies, an inverted microscope (Zeiss, Axiovert 100) with a FLUAR 40 $\times$ /1.3NA oil immersion objective was used. Images were taken in 2–10-s intervals with a digital camera (Hamamatsu C4742-95). The excitation light was provided by a TILL Photonics Monochromator (Polychrome II) tuned to 480 nm. All devices were controlled by the Openlab software (Version 2.3, Improvion) running on a Macintosh G3 computer. Confocal time-lapse sequences were recorded on a Leica TCS SP2 system using a PL FLUOTAR 40 $\times$ /1.0NA oil immersion objective.

#### cAMP Stimulation

cAMP injection experiments in slugs were performed as described [34]. Slugs were prepared as described above, with the cAMP electrode then pushed through the agar. For cAMP pulsing experiments, aggregation-competent cells were allowed to settle on a glass coverslip in the Attofluor chamber and were stimulated with  $5 \times 10^{-6}$

M cAMP (final concentration). cAMP gradients were generated using a gradient maker (BDH) that was filled with KK2 and  $10^{-6}$  M cAMP dissolved in KK2 buffer. Cells were mounted in a perfusion chamber (FCS2, Biopetech) and were perfused with either KK2 buffer or cAMP gradient at a flow rate of  $\sim 1.5$  ml/min.

#### Image Processing and Analysis

For analysis, images were saved in the TIFF format and were transferred to a PC running the Optimas (version 6.1, MediaCybernetics) program. To visualize the waves of CRAC membrane translocation graphically in a cell population, the following procedure was followed. First, the original images were smoothed by applying a  $11 \times 11$  average filter five times. The filtered image was then subtracted from the original image. If cells don't show any membrane localization, this procedure simply reduces the contrast of the image and corrects for uneven illumination. However, if CRAC localizes to the membrane, the background subtraction enhances the cell outline as it acts as a high-pass filter [35]. The average intensity of all pixels of the image or a defined area is then calculated and plotted versus time. At the single cell level, the kinetics of membrane localization were determined by measuring the average brightness in a  $5 \times 5$  or  $10 \times 10$  pixel area over a part of the plasma membrane. The duration of CRAC-GFP membrane binding in vivo for a particular cell was determined by counting the number of images with clear signs of plasma membrane localization.

#### Supplementary Material

Supplementary Material including movies of the experiments described in Figures 1–7 is available at <http://images.cellpress.com/supmat/supmatin.htm>.

#### Acknowledgments

This work was supported by a program grant from the Wellcome Trust to C.J.W.

Received: March 27, 2002

Revised: May 24, 2002

Accepted: May 29, 2002

Published: July 23, 2002

#### References

1. Locascio, A., and Nieto, M.A. (2001). Cell movements during vertebrate development: integrated tissue behaviour versus individual cell migration. *Curr. Opin. Genet. Dev.* **11**, 464–469.
2. Parent, C.A., and Devreotes, P.N. (1999). A cell's sense of direction. *Science* **284**, 765–770.
3. Servant, G., Weiner, O.D., Herzmark, P., Balla, T., Sedat, J.W., and Bourne, H.R. (2000). Polarization of chemoattractant receptor signaling during neutrophil chemotaxis. *Science* **287**, 1037–1040.
4. Firtel, R.A., and Chung, C.Y. (2000). The molecular genetics of chemotaxis: sensing and responding to chemoattractant gradients. *Bioessays* **22**, 603–615.
5. Hirsch, E., Katanaev, V.L., Garlanda, C., Azzolino, O., Piro, L., Silengo, L., Sozzani, S., Mantovani, A., Altruda, F., and Wymann, M.P. (2000). Central role for G protein-coupled phosphoinositide 3-kinase gamma in inflammation. *Science* **287**, 1049–1053.
6. Li, Z., Jiang, H., Xie, W., Zhang, Z., Smrcka, A.V., and Wu, D. (2000). Roles of PLC-beta2 and -beta3 and PI3Kgamma in chemoattractant-mediated signal transduction. *Science* **287**, 1046–1049.
7. Dormann, D., Vasiev, B., and Weijer, C.J. (2000). The control of chemotactic cell movement during *Dictyostelium* morphogenesis. *Philos. Trans. R. Soc. Lond. B. Biol. Sci.* **355**, 983–991.
8. Weijer, C.J. (1999). Morphogenetic cell movement in *Dictyostelium*. *Semin. Cell Dev. Biol.* **10**, 609–619.
9. Parent, C.A., Blacklock, B.J., Froehlich, W.M., Murphy, D.B., and Devreotes, P.N. (1998). G protein signaling events are activated at the leading edge of chemotactic cells. *Cell* **95**, 81–91.
10. Insall, R., Kuspa, A., Lilly, P.J., Shaalsky, G., Levin, L.R., Loomis, W.F., and Devreotes, P. (1994). CRAC, a cytosolic protein containing a pleckstrin homology domain, is required for receptor and G protein-mediated activation of adenylyl cyclase in *Dictyostelium*. *J. Cell Biol.* **126**, 1537–1545.
11. Meili, R., Ellsworth, C., Lee, S., Reddy, T.B.K., Ma, H., and Firtel, R.A. (1999). Chemoattractant-mediated transient activation and membrane localization of Akt/PKB is required for efficient chemotaxis to cAMP in *Dictyostelium*. *EMBO J.* **18**, 2092–2105.
12. Chung, C.Y., Potikyan, G., and Firtel, R.A. (2001). Control of cell polarity and chemotaxis by Akt/PKB and PI3 kinase through the regulation of PAKa. *Mol. Cell* **7**, 937–947.
13. Chung, C.Y., Funamoto, S., and Firtel, R.A. (2001). Signaling pathways controlling cell polarity and chemotaxis. *Trends Biochem. Sci.* **26**, 557–566.
14. Siegert, F., and Weijer, C. (1989). Digital image processing of optical density wave propagation in *Dictyostelium discoideum* and analysis of the effects of caffeine and ammonia. *J. Cell Sci.* **93**, 325–335.
15. Tomchik, K.J., and Devreotes, P.N. (1981). Adenosine 3',5'-monophosphate waves in *Dictyostelium discoideum*: a demonstration by isotope dilution-fluorography technique. *Science* **212**, 443–446.
16. Dormann, D., Abe, T., Weijer, C.J., and Williams, J. (2001). Inducible nuclear translocation of a STAT protein in *Dictyostelium* prespore cells: implications for morphogenesis and cell-type regulation. *Development* **128**, 1081–1088.
17. Brenner, M., and Thoms, S.D. (1984). Caffeine blocks activation of cyclic AMP synthesis in *Dictyostelium discoideum*. *Dev. Biol.* **101**, 136–146.
18. Siegert, F., and Weijer, C.J. (1995). Spiral and concentric waves organize multicellular *Dictyostelium* mounds. *Curr. Biol.* **5**, 937–943.
19. Devreotes, P.N., Potel, M.J., and MacKay, S.A. (1983). Quantitative analysis of cyclic AMP waves mediating aggregation in *Dictyostelium discoideum*. *Dev. Biol.* **96**, 405–415.
20. Dormann, D., and Weijer, C.J. (2001). Propagating chemoattractant waves coordinate periodic cell movement in *Dictyostelium* slugs. *Development* **128**, 4535–4543.
21. Rietdorf, J., Siegert, F., and Weijer, C.J. (1996). Analysis of optical-density wave-propagation and cell-movement during mound formation in *Dictyostelium discoideum*. *Dev. Biol.* **177**, 427–438.
22. Patel, H., Guo, K.D., Parent, C., Gross, J., Devreotes, P.N., and Weijer, C.J. (2000). A temperature-sensitive adenylyl cyclase mutant of *Dictyostelium*. *EMBO J.* **19**, 2247–2256.
23. Jin, T., Zhang, N., Long, Y., Parent, C.A., and Devreotes, P.N. (2000). Localization of the G protein beta gamma complex in living cells during chemotaxis. *Science* **287**, 1034–1036.
24. Zhang, N., Long, Y., and Devreotes, P.N. (2001). Ggamma in *Dictyostelium*: its role in localization of gbetagamma to the membrane is required for chemotaxis in shallow gradients. *Mol. Biol. Cell* **12**, 3204–3213.
25. Janetopoulos, C., Jin, T., and Devreotes, P. (2001). Receptor mediated activation of heterotrimeric G proteins in living cells. *Science* **291**, 2408–2411.
26. Rubin, J., and Robertson, A. (1975). The tip of *Dictyostelium discoideum* pseudoplasmodium as an organizer. *J. Embryol. Exp. Morphol.* **33**, 227–241.
27. Verkerke-van Wijk, I., Fukuzawa, M., Devreotes, P.N., and Schaap, P. (2001). Adenylyl cyclase A expression is tip-specific in *Dictyostelium* slugs and directs StatA nuclear translocation and CudA gene expression. *Dev. Biol.* **234**, 151–160.
28. Tsujioka, M., Yokoyama, M., Nishio, K., Kuwayama, H., Morio, T., Katoh, M., Urushihara, H., Saito, T., Ochiai, H., Tanaka, Y., et al. (2001). Spatial expression patterns of genes involved in cyclic AMP responses in *Dictyostelium discoideum* development. *Dev. Growth Differ.* **43**, 275–283.
29. Wang, B., and Kuspa, A. (1997). *Dictyostelium* development in the absence of cAMP. *Science* **277**, 251–254.
30. Anjard, C., Soderbom, F., and Loomis, W.F. (2001). Requirements for the adenylyl cyclases in the development of *Dictyostelium*. *Development* **128**, 3649–3654.
31. Soderbom, F., Anjard, C., Iranfar, N., Fuller, D., and Loomis, W.F. (1999). An adenylyl cyclase that functions during late development of *Dictyostelium*. *Development* **126**, 5463–5471.

32. Sussman, M. (1987). Cultivation and synchronous morphogenesis of *Dictyostelium* under controlled experimental conditions. *Methods Cell Biol.* 28, 9–29.
33. Dormann, D., Siegert, F., and Weijer, C.J. (1996). Analysis of cell movement during the culmination phase of *Dictyostelium* development. *Development* 122, 761–769.
34. Rietdorf, J., Siegert, F., and Weijer, C.J. (1998). Induction of optical density waves and chemotactic cell movement in *Dictyostelium discoideum* by microinjection of cAMP pulses. *Dev. Biol.* 204, 525–536.
35. Russ, J. (1995). *The Image Processing Handbook*, Second Edition, (Boca Raton, Ann Arbor, London, Tokyo: CRC Press).